# Microstructure investigation of hydrothermal damage of aged SMC composites using Micro-computed tomography and scanning electron microscopy

Abir Abdessalem, Sahbi Tamboura, Joseph Fitoussi, Hachmi Ben Daly, Abbas Tcharkhtchi, Fodil Meraghni

# Microstructure investigation of hydrothermal damage of aged SMC composites using Micro-computed tomography and scanning electron microscopy

Abir Abdessalem [a,b,*], Sahbi Tamboura [b], Joseph Fitoussi [a], Hachmi Ben Daly [b], Abbas Tcharkhtchi [a], Fodil Meraghni [c]

[a] *Arts et Metiers Institute of Technology, CNRS, CNAM, PIMM, HESAM Université, PIMM UMR CNRS 8006, 151 Boulevard de l'Hôpital, 75013 Paris, France*

[b] *Laboratoire Mécanique de Sousse, Ecole Nationale d'Ingénieurs de Sousse (ENISo)-Université de Sousse, Pôle Technologique de Sousse, 4054 Sousse, Tunisia*

[c] *Arts et Metiers Institute of Technology, Université de Lorraine, CNRS, LEM3 UMR-CNRS 7554, ENSAM Metz, 4 Rue Augustin Fresnel, 57070 Metz, France*

A B S T R A C T

This paper presents an investigation on the effects of hydrothermal aging on Sheet Molding Compound (SMC) composite. Two different techniques were carried out to study the inner structure of aged SMC composite. Firstly, X-ray micro computed tomography (XμCT) was used to evaluate the changes using 3D images. The results showed cracks in all the composite structure with different shapes and volume in response to the hydrothermal conditions. The cracks results from the build up of an osmotic pressure in microcavities, which is proportional to water concentration. However, it was not possible to quantify separately the hydrothermal induced damage in the studied SMC composite material. Therefore, the XμCT analyzes were supplemented by a microscopic study. This step has been studied in terms of crack density evolution and crack propagation rate. The results obtained by XμCT technique and SEM observations show that the damage increases continuously with time and temperature during aging. The damage was found to be located in the voids contained in the matrix at early stage of aging. Then it is mostly developed into the fiber interface in the form of fiber/matrix interfacial debonding.

## 1. Introduction

Sheet Molding Compound (SMC) composite is largely used in industries as structural materials due to their diverse advantages. Their potential uses is mainly to reduce components weight especially in aerospace and automotive applications [1–3].

Such a material offers a variety of advantages such as fatigue resistance, ease of manufacturing, and high stifness. However, there are concerns with their service life under environnemental conditions. Indeed, atmospheric humidity combined with temperature is one of the most damaging weather conditions which affect the composite materials.

Various physical processes (i.e. osmosis phenomena, differential swelling) may occur during hydrothermal aging [4–6]. The

deterioration of a composite material during a wet ageing is in most of the cases resulted by a water absorption phenomenon depending on temperature, hygrometric rate and the nature of the composite [7]. In this case, moisture absorption can lead also to permanent damage. The transport of water can be facilitated by diffusion inside the matrix, by imperfections within the matrix created during the elaboration (microspace, pores or cracks) or by capillarity along the interface fibre/matrix [3,8–10].

Microcracking and fiber/matrix bondings breakage are typically the first forms of damage to manifest in such materials under extended hot/wet exposure [8–10]. Once cracking has started, the propagation of microcracks is irreparable and leads to the ruin of the material. It proceeds by an osmotic mechanism described in the literature [7,11–14] and generated by the presence of defects such as microcavities.

Another type of damage observed in thermosets polymer composites is blistering. Indeed, when composites are conditionned, absorbed moisture can generate internal pressure called “osmosis pressure”. When the osmosis pressure exceeds the matrix strength, blistering occurs in the form of macrovoids, microcracks, and/or delamination [15,16].

In order to assess the long-term durabily of such materials, the damage process must be precisely characterized.

Several techniques have been used to date to quantify internal degradation in composites, such as cracks and weak interfaces. In their studies, David et al. [17] have employed a form of instrumented impact test, known by “tap test”, to quantify damages in composite structures used for aircraft. Kinra et al. [18] studied the matrix mico-cracks in laminated composites using an ultrasonic backscattering technique. Finally, as the damage is spatially distributed in composite materials due to their complex morphology, X-ray computed tomography technique (XμCT) has become an efficient tool for damage characterization of such materials. The obtained three-dimensional map enable to visualise and to quantify the composite microstructure, such as the spatial distribution of phases and features and their volume fractions. In this contexte, Schilling et al. [19] applied Xray tomography to analyse internal flaws, delamination and microcracking in graphite/epoxy and glass/epoxy composites due to mechanical loads. Awaja et al. [20] have used X-ray tomography technique to assess the effects of accelerated thermal degradation, cracking and microcracking evolution in in epoxy resin composites. Saucedo-Mora et al. [21] monitored the evolution of damage in ceramic fiber reinforced ceramic matrix composites, using digital volume correlation of X-ray tomographs to quantify the deformation and as an aid to crack visualization.

Arif et al [2] have analysed the fatigue damage behavior of injection molded short glass fiber reinforced polyamide-66 composite (PA66/GF30) by X-ray micro-computed tomography to further understand the damage mechanisms and evolution during fatigue loading.

The description of the kinetics and the propagation mechanisms remaining all the same succinct. The key point of this work lies in the understanding of cracking stages, due to hydrothermal conditions, based on experimental study. To this aim, X-ray computed tomography has been carried out to characterize the inner structure of SMC composite at different aging time and temperature. However, this technique was not able to quantify seperately the damages due to hydrothermal conditions. Therefore, the results of X-ray tomography were combined to scanning electron microscopy (SEM) observations in order to quantify seperately the internal damages in the studied aged material, and so to propose hydrothermal degradation scenario of SMC composite.

## 2. Material description, experimental procedure and techniques

### 2.1. Material

The SMC provided by Faurecia campany for this study has a simplified conventional formulation, i.e. 28% glass fibers, 35% calcium carbonate filler ($CaCO_3$), and 37% unsaturated polyester resin. It was moulded on a conventional press, in a rectangular mould equipped with pressure and dielectric sensors. The moulding conditions were: temperature $160 \pm 3\ ^{\circ}C$, pressure $30-100$bars, and duration 3min. Specimens of $60 \times 15 \times 2\ mm^3$ were cut from the tailgate plates with a diamond saw and finished on a polishing machine with water. The cutting template was the same for all experiments.

### 2.2. Experimental procedures

#### 2.2.1. Computed tomography

X-ray computed tomography was adopted to analyse the internal damage of the SMC composite after hydrothermal aging. The absorbance of the X-rays correlates to the density of the specimen examined volume. Since glass fiber, polyester matrix, calcium carbonate fillers, and voids all have a different density, the internal composition and structure can be revealed. A void was defined as an internal cavity filled with air or other gasses where there is no material present. The scans were performed using an X-ray microscope (MicroXCT-400 of LEM3 laboratory). The X-ray tube voltage and current were set to respectively 95 kV and 53 μA. The obtained voxel size was nominally 2,3 μm. The reconstruction software was used to assign a grey value to each volume element, or voxel, and to reconstruct a three dimensional model of the material examined volume. The ageing protocol is described in Section 2.4. For each composite sample, the exact same volume of approximately 6 $mm^3$ was analyzed. The extracted binary images were used to calculate the void content. Quantitative analysis was performed on two specimens for each composite type. The evolution of voids during aging was linked to the development of damage and visualized with Avizo (v9.0).

#### 2.2.2. Electron microscopy (SEM)

Surfaces for microscopy were smoothed by a conventional method with a polishing machine, and then polished with 3 mm diamond powder on a cloth pad; this operation had to be made carefully to avoid any relief difference between the glass fibres and the

matrix. The polishing time has to be as short as possible, using a large flow of fresh water, in order to avoid filling the voids with dust. With the diamond powder, a very careful and short polishing is suitable, even if scratches remain on the surface. A thin metal coating (Au–Pd sputtering) was made prior to examination by scanning electron microscopy (SEM). SEM experiments were performed on a Hitachi 4800 instrument. The corresponding images were, then, processed with Imaging software for porosity measurement and size of the voids. The technique of extracting morphological information from samples during and after acquisition provides digital images, used in the format of 384 × 512 pixels of 8 bits.

### 2.2.3. *Ultrasonic measurement (US)*

Ultrasonic tests were performed to analyse the fiber orientation. This technique consists on immersing two probes in a tank of water, one is made to transmet the ultrasonic waves, denoted probe (E), and a second, denoted probe (R), to receive it. The distance "d" between these two probes is known (measured or imposed) and remains constant along the measurements procedure.

The first step consists on measuring the velocity of wave propagation in water. To this aim, an oscilloscope is used to determine the time $t_0$defined as the time taken by the wave to pass from the probe (E) to the probe (R). Knowing the distance between the two probes, the propagation wave's velocity, denoted $V_0$, can be deduced using the Eq. (1):

$$V_0 = \frac{d}{t_0} \tag{1}$$

In a second step, the composite specimen is placed between the two probes and perpondicular to the ultrasonic path as shown in Fig. 1. Here, the time, denoted $t_e$, taken by the ultrasonic wave to spread the distance "d" is measured.

The velocity of the longitudinal waves in the sample, denoted $V_{OL}$, is so deduced using the following equation:

$$V_{OL} = \frac{e}{t_e - \frac{d-e}{V_0}} \tag{2}$$

where e is the sample thickness.

The sample is, then, rotated by an angle i (incidence angle) to bring up the transversal waves that will propagate throughout the specimen thickness in a direction (r) as shown in Fig. 2. This direction is determined by Snell Descartes' law:

$$\frac{sin(i)}{V_0} = \frac{sin(r)}{V_{OT}} \tag{3}$$

where $V_{OT}$ is the transversal wave velocity in the specimen.

Finally, the transverval velocity, $V_{OT}$, is determinated and is given by the following equation

$$V_{OT} = \frac{eV_0}{\sqrt{e^2 + 2eV_0(t_e - t_0)cos(i) + V_0^2(t_e - t_0)^2}} \tag{4}$$

The variation in transverval velocity, $V_{OT}$, is directly linked to fiber orientation. This is followed by the rotation of the specimen around its normal axis. If the fibers have an orientation in the shear plane as shown in Fig. 2 (a), high values of $V_{OT}$ are recorded. However, if the fibers have a perpendicular orientation as illustrated in Fig. 2 (b), the velocity records lower values.

In addition, an indicator called the acoustic birefringence coefficient and denoted K (%) can be defined from these tests. This coefficient is linked to the "intensity" of fiber orientation and it is given by the following formula:

$$K = \frac{V_{OTmax} - V_{OTmin}}{V_{OTav}} \tag{5}$$

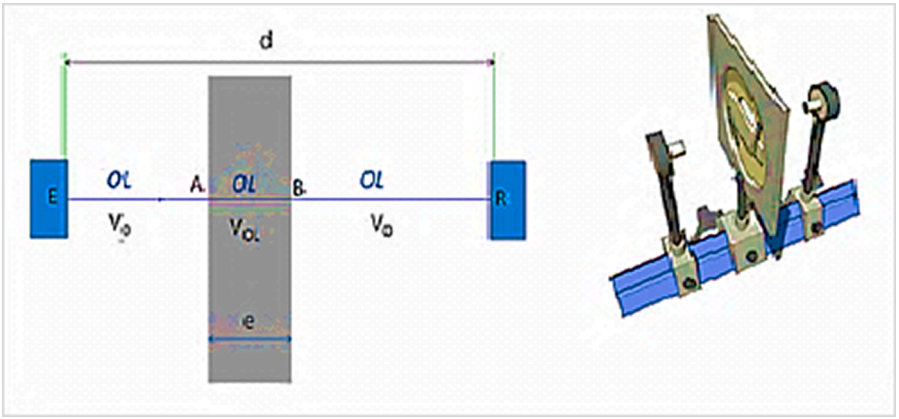


**Fig. 1.** Schematic presentation of the ultrasonic measurement device.

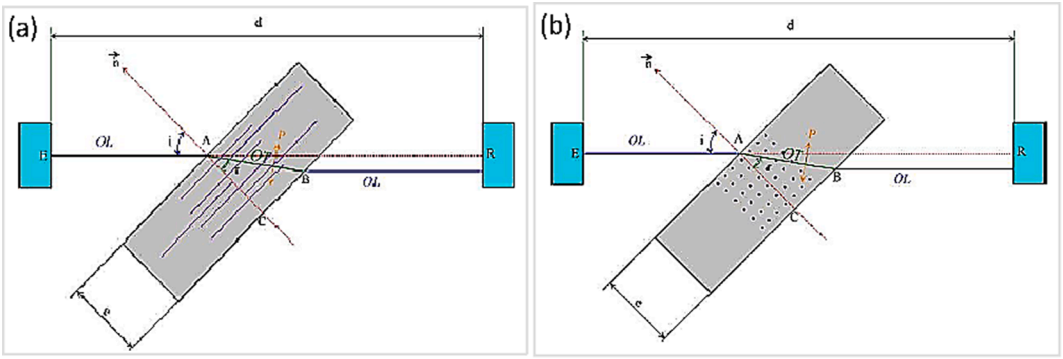


**Fig. 2.** The second step in ultrasonic measurement: determination of fiber orientation.

where $V_{OTav}$ is the average value of $V_{OT}$.

### 2.3. Microstructure analysis

Microscopic observations revealed the usual complex morphology of SMC, with the presence of individual fibres, glass tows in various directions and circular voids due to the residual air in the prepreg as shown in Fig. 3.

Four different elements, i.e. the micro-voids, the matrix, glass fibres and the fillers ($CaCO_3$), can be seen with a grey level specific to each one: dark, grey light grey and white, respectively. So, the image processing is greatly simplified. The microvoids, the matrix the glass fibers and the fillers are segmented by using a simple thresholding. The microporosity is calculated by taking the ratio of the surface of the average microvoids with respect to that of the matrix. The size distributions of the microvoids are obtained by classical binary image processing. It should be noticed that the image is a slice of the material and that the microvoids have complex shapes.

From microscopic images we found, for the non-aged material, porosities 7% ± 0.4% and average diameter of 6.5 $\mu$m to 9 $\mu$m.

Therefore, there is a clear influence of fiber orientation.

The determination of the fiber orientation in the studied SMC composite was carried out on various samples using US tests. The results of the ultrasonic characterization method are illustrated in Fig. 4 (a). As it can be denoted, a preferred orientation of the glass fibers was recorded around 60°. This is proved by the presence of two peaks, one at aroud 60° and its symmetric around 240° corresponding to fiber orientation.

However, the birefringence coefficient records a relative depletion in fibers since its value does not exceed 8% as shown in Fig. 4(b).

### 2.4. Hydrothermal aging conditions

Samples of of SMC compositewere cut and were immersed in water at 25, 50, 70 and 90 °C (±2 °C). The Weight change evolution was recorded periodically, after drying with a soft towel, using a METTLER AT261 balance (with a precision of ±0.05 mg). The moisture content was determined using equation $M_t\ (\%) = \frac{m_t - m_0}{m_0}$ (6) where $m_t$ and $m_0$ denote, respectively, the sample weight at a given time t and the initial specimen weight before exposure.

**Fig. 3.** Microscopic observation of the non-aged sample surface.

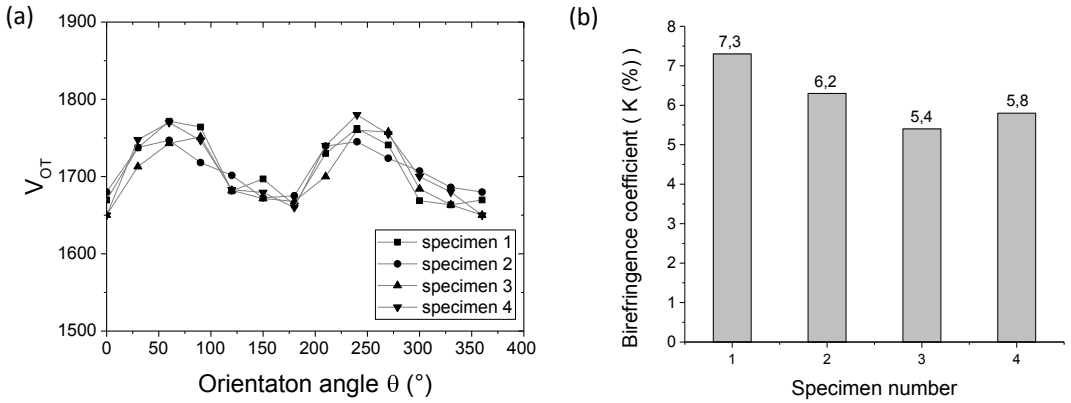


**Fig. 4.** Ultrasonic results showing (a) fiber orientation around 60° and (b) the fiber orientation intensity.

## 3. Results

### *3.1. Gravimetric tests*

The kinetic of water sorption was analysed in the previous study [22]. It was found that water diffusion in SMC composites follows the "Langmuir type diffusion" based on Carter and Kibler's theory [23]. In their theory, Carter and Kibler suppose the existence of two types of water molecules in the material, «mobile» and «bound». The «mobile» and «bound» water molecules are respectively the free or the non-hydrogen bounded molecules and the hydrogen bounded molecules.

The Langmuir diffusion in based on the equations below:

$$\frac{n(t)}{M} = \frac{\beta}{\beta+\gamma}\left\{1 - \frac{8}{\pi^2}e^{-kt}\right\} \tag{7}$$

$$\frac{N(t)}{M} = \frac{\gamma\beta}{\beta+\gamma}e^{-\beta t}\left\{\frac{1}{\beta}(e^{\beta t}-1) - \frac{8}{\pi^2 k}(e^{-kt}-1)\right\} \tag{8}$$

where $N(z,t) and n(z,t)$ are the bound and free water molecules respectively, M is the total number of water molecules at time t $(M(t) = n(t) + N(t))$, $\gamma$ and $\beta$ are respectively the probabilities that a water molecule is presented in the form of hydrogen-bounded and mobile. The results obtained on 90 °C aged samples are shown in Fig. 5 where the normalized water uptake data (as mass uptake/mass at saturation) are plotted versus the normalized time given by $t^{0.5}/e$ (where e is the sample thickness). Similar trends were obtained for samples aged at 25, 50 and 70 °C and can be found here [22].

It was found that the «mobile» water corresponding to the diffusion in the micro-porosities. Whereas the «bound» water, refers to crosslinking and plasticization effect.

The mass variation shows three behaviors. Firstly, for all the specimens, the water absorption process is linear and $\left(\frac{M_t - M_0}{M_0}\right) > 0$.

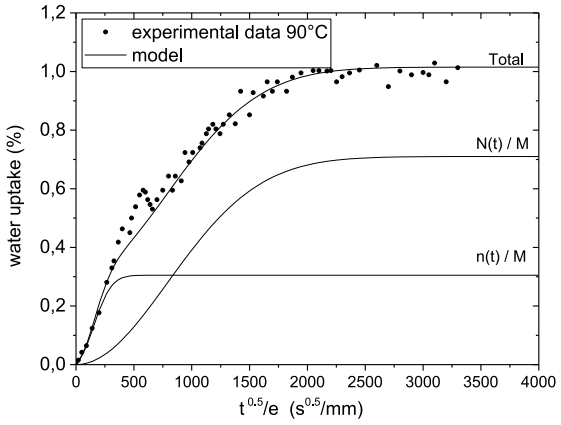


**Fig. 5.** Gravimetric results for water absorption at 90 °C. (●) experimental, (−) model.

Then a decrease, at shifted periods of time, was recorded on the absorption curves where $\frac{M_t - M_0}{M_0} < 0$. This phenomenon was associated to the leaching of the calcium carbonate fillers due to water attack. Finally, the diffusion restarts again in the material until the saturation.

In this study, we are interested to discuss the effect of mobile water molecules diffusion in the SMC microstructure. The effect of hydrogen-bounded molecules were discussed in the previous work [22].

### 3.2. *Effect of hydrothermal aging on the damage*

The outer surfaces of aged samples at 25 °C, 50 °C, 70 °C and 90 °C were visually contrôled during the hydrothermal conditionning. Fig. 6 shows the external surfaces aspects of aged specimens after 500 h and 2500 h in tempered water. Blisters appear in the exposed surfaces, and their kinetics is accelerated with time and temperature.

After 500 h in water, the blisters size is more and more marked when the aging temperature is close to the glass transition temperature of the polyester resin used in this work ($T_g = 91\ ^\circ C$) as it can be seen in Fig. 6(a). However, at 50 °C and 25 °C, the blistering phenomenon does not occur since at these temperatures the material is in a glassy state. It will probably appear for much longer immersion times. Otherwise, it can be noted that the increase in immersion time from 500 h to 2500 h increases the number of blisters as shown in Fig. 6(b).

This result is actually expected. Indeed, increasing the immersion parameters (time and Temperature) increases both the diffusion and the amount of moisture introduced into the sample. Over time, the pressure of the water inside the material, called osmotic pressure, increases and can, thus, reach a critical value giving rise to local damage. It was very recognized that blistering induced by humid aging is a very important mode of failure in these materials [7]. That is the reason why it became of major interest to understand the microcrack nucleation mechanism in SMC composite in order to study their propagation and to quantify their evolution.

#### 3.2.1. *Damage analysis based on X-ray micro-computed tomography*

The XμCT was performed to visualize and understand the 3D damage evolution during hydrothermal conditions. In Figs. 7 and 8, three-dimensional reconstructions of a 50 °C and 90 °C aged samples after three water uptake levels (15%, 30% and 60%) are shown. The focus was put on the inner parts to visualize the most important damage mechanisms namely matrix cracking and fibre–matrix debonding.

In Fig. 9, cross sections of the 90 °C aged composite after different water uptake are shown. Overall, the damage development in the aged SMC composite proceeded faster which is in line with the evolution in water uptake properties as discussed in the previous work [22].

Before ageing, mainly cylindrical dark features appear which correspond to the naturally present voids. Moreover, a good adhesion between the the fiber and the matrix is marqued.

At low water uptake (15% $M_s$), matrix cracking have occurred which are often attributed in literature to osmotic stresses due to the water molecules diffusion in mico-voids during immersion [24]. This damage is much more marked at high temperature.

At 30% of water uptake, significant damage were emerged and propagates in fibre direction in sampples aged at 90 °C. Cracks appeared at the interface between the matrix and the fiber, as shown in Fig. 9. The interface detachment developed and progressed in the form of long crack as the hygrothermal aging time was increased. Interface cracking is a result of failure of the internal interfaces [20]. However, only few micro-cracks appear in the inner structure of 50 °C aged samples at this water uptake level.

At high water uptake (60% $M_s$), the fibre/matrix bond weakened with the increase of the moisture content. Fibre-matrix debonding occurred at the edges of the fibre bundles. The fibre–matrix debonding and splitting of the fibre bundle are the predominant damage mechanism suggesting that the majority of the damage occurs during aging at high temperatures. This might indicate that the long-term aging strengthens the damage progress. However, the moisture diffusion did not seem to have had a large influence on the quality of the fiber/matrix interface at low temperatures. Significant interfacial degradation have occurred only after a long exposure to moisture.

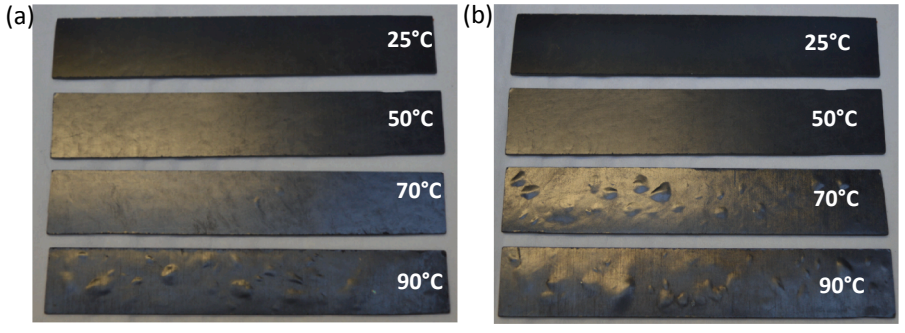


**Fig. 6.** appearence of blisters on the outer surfaces of aged SMC samples (a) after 500 h, (b) after 2500 h in water immersion at 25 °C, 50 °C, 70 °C and 90 °C.

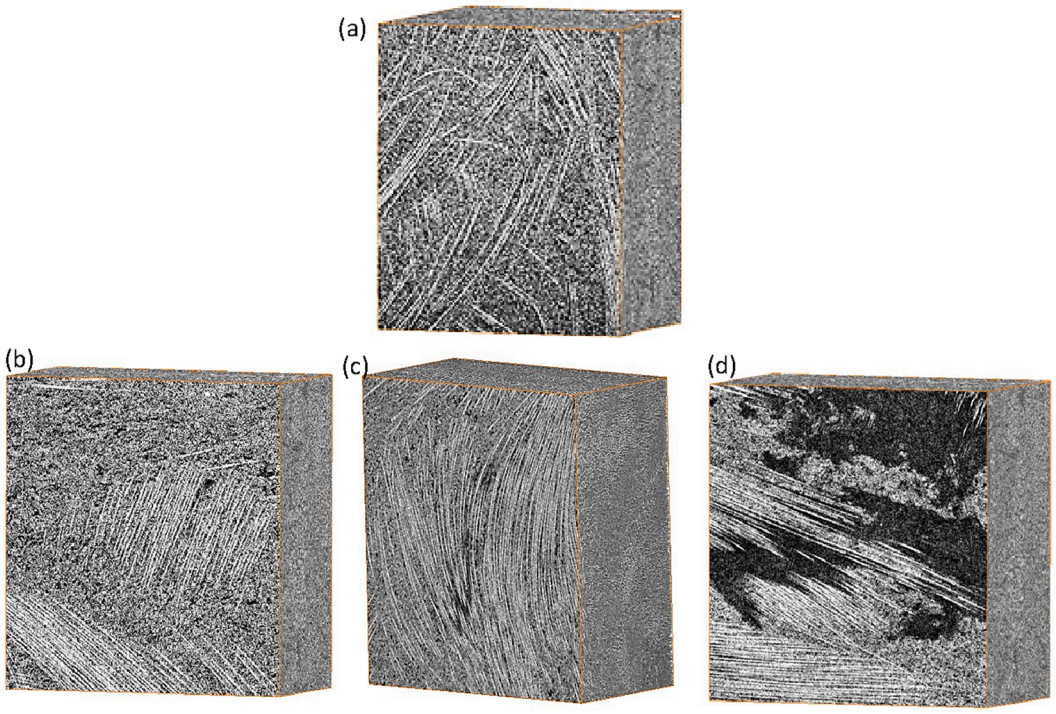


**Fig. 7.** 3D damage observation of (a) non aged sample, and 90 °C aged SMC samples after (b) 15% $M_S$, (c) 30% $M_S$, and (d) 60% $M_S$.

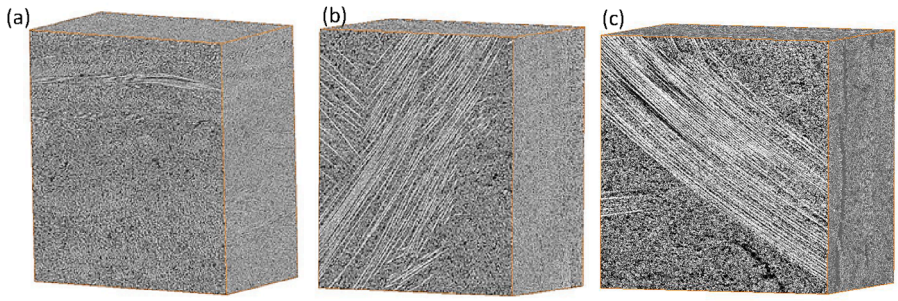


**Fig. 8.** 3D damage observation of 50 °C aged SMC samples after (a) 15% $M_S$, (b) 30% $M_S$, and (c) 60% $M_S$.

In Fig. 10, quantitative data of the increase in voids during the hygroscopic ageing is shown.

It was supposed that the initial void fraction corresponds to the defects present in the material before conditionning. The increase in voids was attributed to the development of damage. The calculated increase is prone to error which could be a result of small variations in image quality, segmentation and examined volume.

Both the quantitative and visual analysis indicate that there was a clear influence of the water diffusion. The tomographic results revealed that specimens experienced harsher damaging when exposed to hot/wet aging condition suggesting that the temperature as an environmental factor play an accelerating role for damage mechanism of SMC composite under hydrothermal aging. However, with XμCT it was not possible to study seperately the identified damages during aging. Detailed future analysis of the damages with scanning electron microscopy might point out seperately the evolution of each identified hydrothermal damage.

*3.2.2. Damage analysis based on SEM images*

The XμCT provided informations about the microstructure and SEM further elaborated the comprehensive information about matrix, fibres and fibre/matrix interfaces.

In this study, Scanning Electron Microscopic (SEM) observations were made to study in detail the process of crack initiation and crack propagation in a short fibre-reinforced composite under hydrothermal environment.

The surface of non-aged samples and aged at 25 °C, 50 °C, 70 °C and 90 °C were analysed after respectively 15%, 30% and 60% of water uptake. For brevity, we only show the results of 50 °C and 90 °C aged samples.

In this study, damages were found to be dependent on time, temperatures and moisture content. Since moisture cannot penetrate

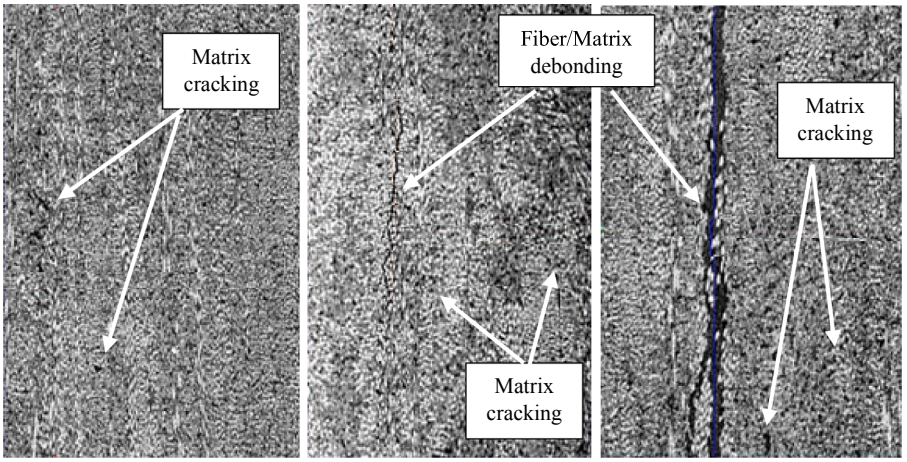


**Fig. 9.** Cross-section of 90 °C conditionned SMC composite after (a) 15% $M_S$, (b) 30% $M_S$, and (c) 60% $M_S$.

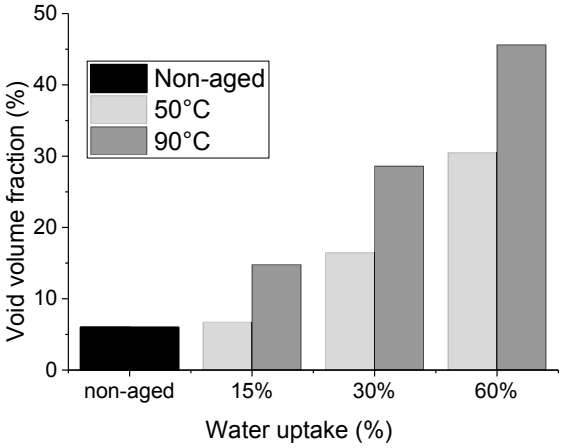


**Fig. 10.** Evolution of the void volume fraction of non aged sample and 50 °C and 90 °C aged samples versus the water uptake level.

fibers, the behavior of diffusing moisture in composites is usually affected by the resin properties.

As it can be seen in Fig. 11, the effect of hydrothermal ageing is clear: i.e. a visible increase of the amount of voids/porosities.

Cracks within the matrix were observed when conditionning at all aging temperatures which was a consequence of water molecules diffusion to the free volume spaces and porosities. However, cracks within fiber/matrix interface were found to be dependent on time, temperatures and moisture content. Indeed, for low immersion temperature (25 °C and 50 °C) and low humidity centent (15% $M_S$), no visible damages were deceted in the aged samples. When increasing the humidity content (30% $M_S$), large size porosities in the matrix area were noted, followed by a weak interfacial cohesion which becomes more significant at relatively high humidity content (60% $M_S$).

However, at high immersion temperatures (70 °C and 90 °C), we noted, in addition to the matrix degradation, a very significant interfacial damage starting at low humidity content (15% $M_S$). Then, clean and smooth surfaces of pulled out fibers were found for 60% $M_S$ indicating that the SMC composite was extensively attacked under hot-wet conditions.

When comparing the SEM observations of aged and non-aged samples, three types of damages have been distinguished:

Class A: matrix osmotic cracking
Class B: interfacial debonding. It may be induced by differential swelling or by osmotic cracking at the interphase. As a matter of fact the interfacial zone constitutes a privileged site for osmosis process because of stress concentration in these zones. The consequence of such a process is cracking along or between fibre mesh.
Class C: inter-wick cracks taking place between two differently oriented wicks.

In the following, the three identified damages are analysed and quantified seperately.

***Class A:***

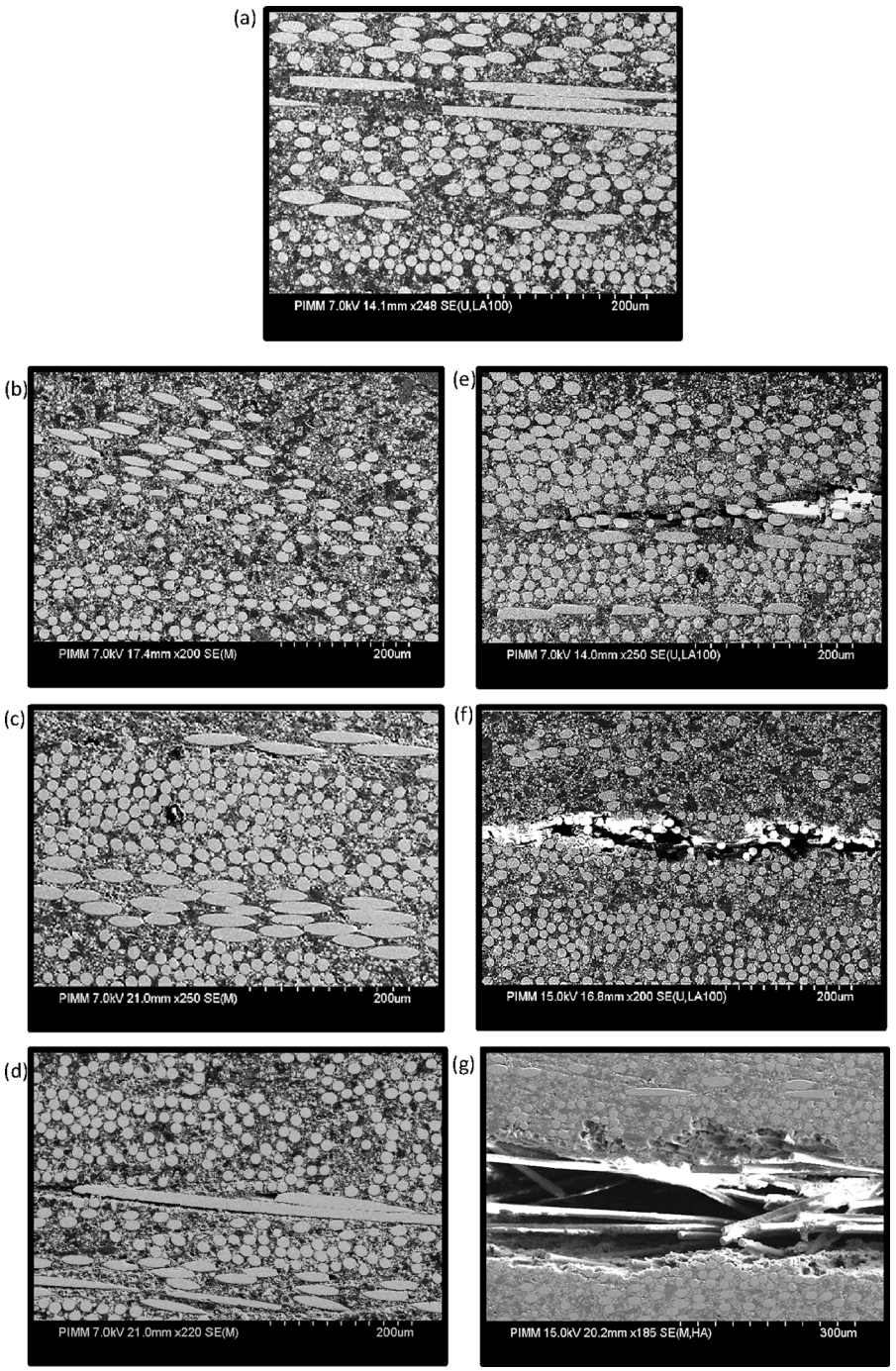


**Fig. 11.** SEM micrographs of the inner microstructure evolution of the (a) non aged sample, (b)–(d) 50 °C aged samples after respectively 15% $M_S$, 30% $M_S$, and 60% $M_S$, and (e)–(g) 90 °C aged samples after respectively 15% $M_S$, 30% $M_S$, and 60% $M_S$.

In a composite material, the matrix acts as a semi-permeable membrane, and it is suspected to play a key role in osmotic pressure build up. Cracks within polymer matrix are, generally, associated to local damage produced by water diffusion in the heterogeneities pre-existing in the polymer network which are essentially micro-porosities that are the origin of air bubbles, soluble impurities, or defects.

The matrix osmotic cracking was performed by following the voids densities over the aging time at the four studied temperatures. The porosities density were estimated using Eq. (9)

$$D_v = \frac{n_P * S_P}{RES} \tag{9}$$

where $D_v$, $n_p$ and $S_p$ are respectively the density, the number and the average surface of a porosity and RSE is a representative elemntary surface.

The results of this method are shown in Fig. 12.

It is clear that the more the immersion parameters (time, Temperature) have increased, the more the density of the cavities displayed in the matrix increases. This growth is linked to the increase in the amount of the diffused moisture into the sample which results essentially in:

- An increase in the porosities sizes due to an increase in the osmotic pressure inside these sites.
- An increase in the number of porosities caused by the phenomena of the chalks particules leaching; i.e this phenomena was discussed and analysed in the previous work [22].

***Class B:***

The SEM observations previously illustrated showed also the appearance of cracks at the fiber/matrix interface which play an important role in increasing water molecules penetration.

The growth of these interfacial cracks during water immersion was controlled by the evolution of their densities. Indeed, for a given orientation of the fibers, denoted θ, the density of interfacial cracks ($D_{in}$) is estimated as being the ratio between the number of loose fibers ($N_f$) belonging to an oriented wick and the total number of fibers contained in the same oriented wick ($N_m$). This is described by the following equation:

$$D_{in} = \frac{N_f}{N_m} \tag{10}$$

Thus this analysis is not simple: the information has to be extracted at every oriented wick. However, with the use of average oriented wick, such an analysis may be done. In this case, we were first interested in fibers oriented between 30° and 60° to characterize an average density denoted by d_45°, and in a second time we studied fibers oriented between 65° and 90° to characterize an average density denoted by d_90°.

From these two densities, we have defined an overall interfacial debonding density, dnoted d_global, which is the sum of d_45° and d_90°.

The results of this method is shown in Fig. 13.

Fibre-matrix debonding occurred at the edges of the fibre bundles which is a result of water attack and stresses accumulating at the interface during sorption. Cracking of the fibre bundles is a result of failure of the internal interfaces. We can notice that the interfacial crack density, d_global, increases with aging parameters (t, T). Such irreversible structural change is consistent and it is linked to the build-up of the critical stress inside the fibre bundle due to moisture sorption.

***Class C:***

In the same way, we defined an inter-wick crack density as follow:

$$D_I = \frac{n_I * S_I}{RES} \tag{11}$$

where $D_I$, $n_I$and$S_I$ are respectively the density, the number and the surface of the inter-wick crack, RES is a representative elemntary

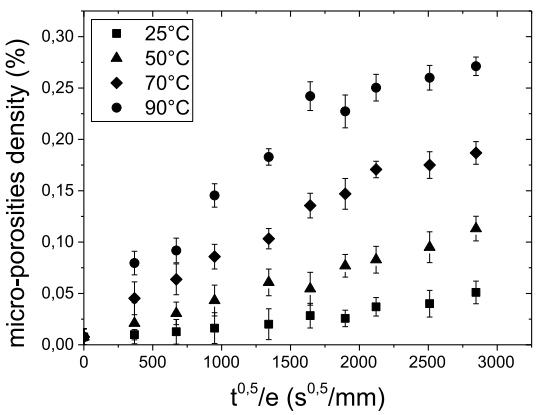


**Fig. 12.** Micro-porosities density evolution at 25 °C, 50 °C, 70 °C and 90 °C aver aging time.

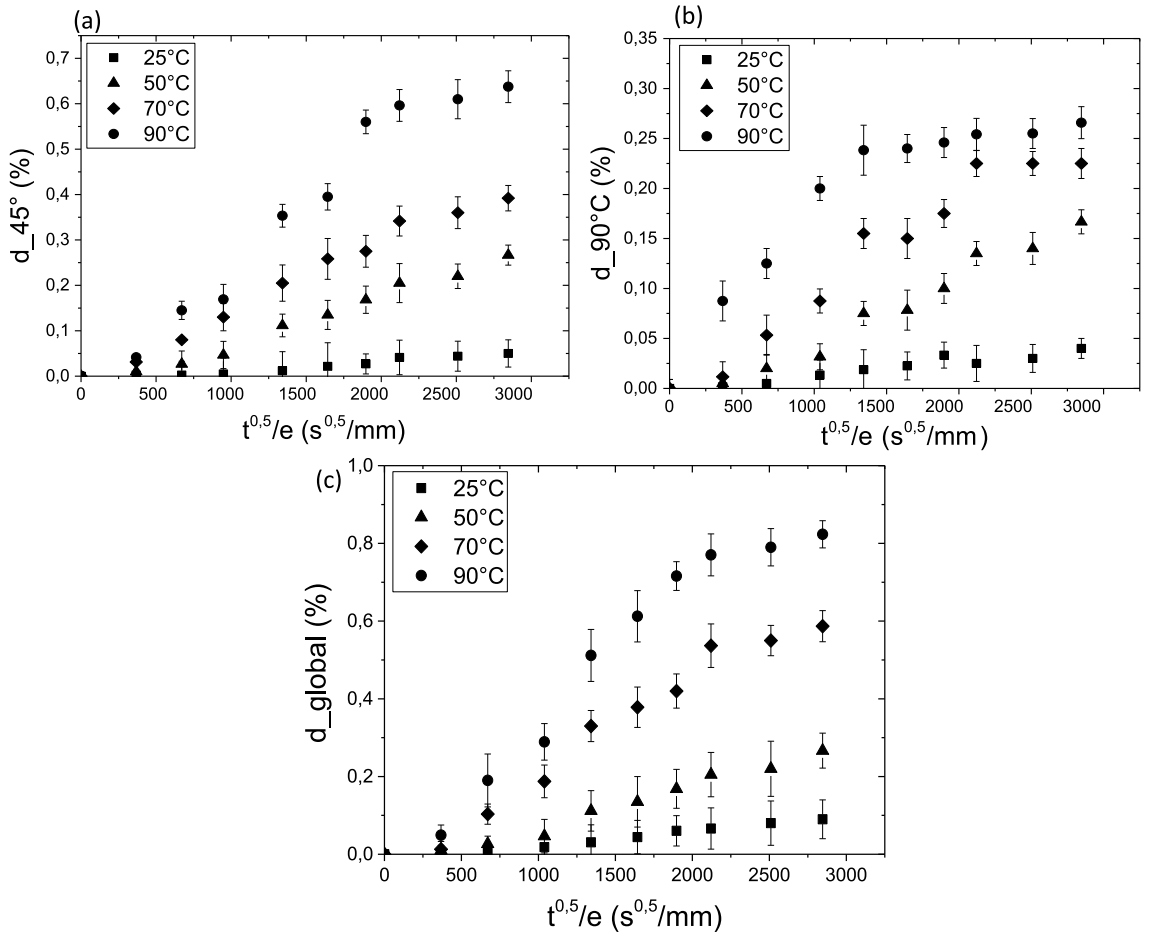


**Fig. 13.** Interfacial crack evolution associated to (a) 45° oriented glass fibers, (b) 90° oriented glass fibers and (c) the global density at 25 °C, 50 °C, 70 °C and 90 °C aver aging time.

surface.

The obtained results, illustrated in Fig. 14, highlight a weak trend in the inter-wick cracks evolution compared to matrix cracking and interfacial degradation. The inter-wick cracks were observed only on specimens exposed to 90 °C and 70 °C in water immersion and after an extended aging period. Small fracture were observed in samples aged at 50 °C. However, no inter-wick cracks were observed at 25 °C. It will probably appear for much longer immersion times.

### *3.3. Discussion*

Humid aging was recognized as one of the main causes of long-term failure of organic matrix composite. Once immersed in distilled water, the moisture diffuses by capillarity by the Carter and Kibler's theory into the sample containing porosities according to the concentration principle. In the studied material, the diffused water molecules are present in two types. We distinguish, from one hand, the free water molecules which can diffuses only in the available spaces (free volume/porosities), and from the other hand, the bound water molecules defined as hydrogen-bonded molecules which appear when the intermolecular bonds (hydrogen and Van Der Waals bonds) are broken due to the plasticization effect.

In our previous study, we have shown that the amount of free water present in aged samples is more important than the bounded phase. The amount of absorbed free water increases with the immersion parameters (t, T). Indeed, the temperature contributes to a significant excitation of water molecules, allowing them to acquire an increasingly important kinetic energy. This allows water to diffuse more easily and quickly into the sample.

If the composite material contains minerals as reinforcing particles phase such as calcium carbonate, the diffusion of moisture in such a material is, then, accelerated due to the hydrophilic nature of these particles. In this case, water can also act on the polymer/chalk interface, promoting the detachment of chalks from the matrix and subsequently their migrations towards the external surface of the sample.

With the increase in the moisture sorption over time, the pressure inside the free volumes, porosities and fiber/matrix interfaces

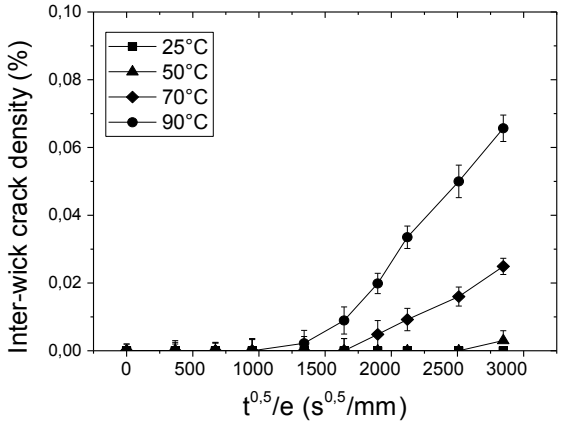


**Fig. 14.** Evolution of the inter-wick cracks density over time at different temperatures.

gradually increases. Consequently, this leads to a growth in the size of these defects which, in several cases, favors either their propagation or their coalescence, or even the two phenomena simultaneously.

The damages caused by aging were well observed in the matrix and the fibre/matrix interface.

The occurrence of matrix damage is the fisrt observed process of failure in the SMC microstructure under hydrothermal conditions. As the matrix acts as a semipermeable membrane, the permeability to water molecules, suspected to play a key role in osmotic pressure build up. When the water uptake level was increased, a cluster of microcracks was generated in the matrix which is the first indication of hydrothermal failure. That crack initiation is linked to the presence of water molecules in the network and the heterogeneities pre-exist in the matrix which may be microporosities induced by manufacturing process. These molecules would accumulate in these sites thus creating highly liquid micropockets able to initiate osmotic cracking. However, in his study, Gautier [7] showed that the effect of water on the unsaturated polyester resin is to close the microvoids in the core of the material, which is not the case in this study.

Furthermore, during the moisture absorption a generation of interfacial microcracks in the matrix along the fiber side was observed. The microcracks generated at the initial stage of aging showed little growth under the elevated temperature. The interphase becomes an absorption site because of interfacial debonding as a result of matrix swelling. Therefore, water molecules settled down in the macro voids formed by cavities and cracks, which induced further cavities and cracks, thus the interphase was gradually damaged. The occurrence of interfacial cracks at the fibre side is thought to be the second process of failure. The detailed failure analysis revealed that it is the dominated hydrothermal fracture.

These interfacial cracks and matrix cracks may result in a catastrophic crack propagation in the composite. Propagation results can be interpreted in terms of osmotic process and can be schemed as shown in Fig. 15.

The initiation and growth of the cracks are interpreted on the basis of osmotic stress distribution as follow: under immersion, water molecules diffuses preferably in the the heterogeneities pre-exist in the matrix. Therefore, the stress concentration occurs, firstly, in these sites. The accumulation of water molecules inside these sites increases the osmotic pressure. At a critical value, the microcrack size increases, thus leading to an increase in water sorption and therefore to an osmotic pressure. This pressure stabilizes the micropocket size until the osmotic pressure reaches a critical value. Therefore, the occurrence and the growth of the crack increases the concentrated stress in the voids and at the interfaces as water molecules diffuses largly in these sites, and further the micocrack growth

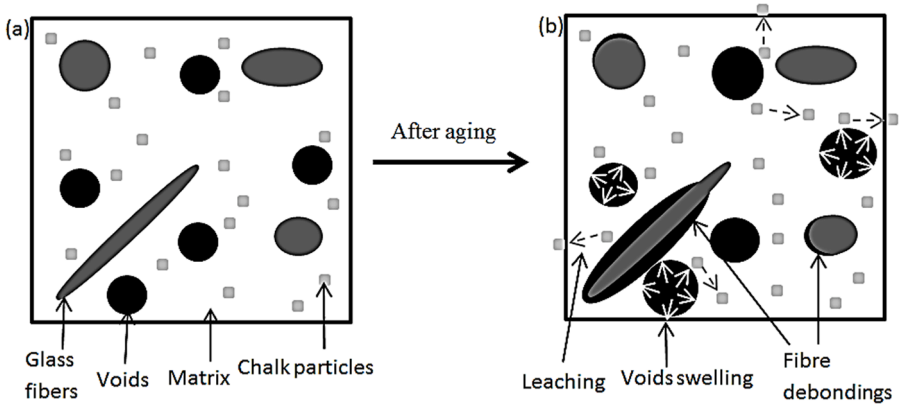


**Fig. 15.** Schematic description of swelling and leaching of $CaCO_3$ particles due to water diffusion in the existent voids (a) initially before aging and (b) after aging.

will be encouraged. The resultant high stress causes interaction of stresses between neighbouring interfacial cracks, and the band of microcracks connecting fibres will be generated. The osmotic interface damage appears therefore responsible for the material degradation.

## 4. Conclusions

This study presented the effect of hydrothermal aging on the morphology of glass fibre reinforced polyester composite. This is of major interest for many applications in order to warranty lifetime in service. From this investigation it can be conclude that:

- The moisture diffusivity followed a typical two-types model called Langmuir type diffusion where water absorption diffuses in the material and be presented either mobile or hydrogen-bounded. Here in this study we were interested to the mobile water phase.
- Increasing the ageing parameters (time and temperature) effects the morphological aspect of the material. Detailed failure analysis by XμCT revealed an increase in fracture densities in the aged SMC composite over time under humid tempered environment. However, it was not possible to analyse seperately the different observed damages.
- SEM observations were, thus, carried out to quantify seperately the hydrothermal damages. The obtained analysis are interesting for two reasons. First, the degraded microstructure is well resolved. Second, the damage appears to be clearly observed. Therefore, three types of damage processes have been distinguished, namely osmotic cracking which may occur either inside the matrix or at the interface, and interfacial debonding. They have been considered seperately to follow their propagations and to quantify their densities. It have been shown that, at early aging periods, the first fracture of the aged SMC was matrix dominated. Then, cracking between the fiber and matrix due to differential swelling and weakening of the interface were observed. It was shown that the interfacial cracks has a significant detrimental effect as its density is the most important compared to the matrix crack density.
- Finally, we may conclude that during hydrothermal ageing SMC composite, matrix degradation occurs through an osmotic process. Once the micropocket has been initiated, the cavity size increases according to an osmotic process. The crack propagation proceeds by a nucleation/spreading mechanism, meaning that both crack density and crack length increase. The main characteristic of crack propagation is the crack propagation rate that is governed by the temperature and the critical osmotic pressure required for the crack to propagate. These parameters explain the difference observed in the propagation rates.

The effect of moisture or water on the properties of polymer composites is an important issue and that is why further study is necessary. In this context, a future study is recommended to examine the effects of moisture and temperature on mechanical behaviour such as tensile properties and fatigue behaviour.

## Declaration of Competing Interest

The authors declare that they have no known competing financial interests or personal relationships that could have appeared to influence the work reported in this paper.

## Acknowledgments

This work is supported by Ecole des Arts et Metiers – France and Ecole Nationale d'Ingénieurs de Sousse – Université de Sousse – Tunisie.

## References

[1] S.T. Peters, Handbook of Composites, Springer Science & Business Media, 2013.
[2] M.F. Arif, N. Saintier, F. Meraghni, J. Fitoussi, Y. Chemisky, G. Robert, Multiscale fatigue damage characterization in short glass fiber reinforced polyamide-66, Compos. B Eng. 61 (2014) 55–65.
[3] L. Gautier, B. Mortaigne, V. Bellenger, Interface damage study of hydrothermally aged glass-fibre-reinforced polyester composites, Compos. Sci. Technol. 59 (16) (1999) 2329–2337.
[4] J.F. Berthet, E. Ferrier, P. Hamelin, Compressive behavior of concrete externally confined by composite jackets. Part A: experimental study, Constr. Build. Mater. 19 (3) (2005) 223–232.
[5] Y. Joliff, L. Belec, M.B. Heman, J.F. Chailan, Experimental, analytical and numerical study of water diffusion in unidirectional composite materials – Interphase impact, Comput. Mater. Sci. 64 (2012) 141–145.
[6] J. Zhou, J.P. Lucas, Hygrothermal effects of epoxy resin. Part I: the nature of water in epoxy, Polymer 40 (20) (1999) 5505–5512.
[7] L. Gautier, B. Mortaigne, V. Bellenger, J. Verdu, Osmotic cracking nucleation in hydrothermal-aged polyester matrix, Polymer 41 (7) (2000) 2481–2490.
[8] A. Tcharkhtchi, P.Y. Bronnec, J. Verdu, Water absorption characteristics of diglycidylether of butane diol–3,5-diethyl-2,4-diaminotoluene networks, Polymer 41 (15) (2000) 5777–5785.
[9] C. Carfagna, A. Apicella, Physical degradation by water clustering in epoxy resins, J. Appl. Polym. Sci. 28 (9) (1983) 2881–2885.
[10] L. Burcham, M. Vanlandingham, R. Eduljee, J. Gillespie Jr., Moisture effects on the behavior of graphite/polyimide composites, Polym. Compos. 17 (1996) 682–690.
[11] Z.A. Mohd Ishak, U.S. Ishiaku, J. Karger-Kocsis, Hygrothermal aging and fracture behavior of short-glass-fiber-reinforced rubber-toughened poly(butylene terephthalate) composites, Compos. Sci. Technol. 60 (6) (2000) 803–815.
[12] A.E. Scott, I. Sinclair, S.M. Spearing, M.N. Mavrogordato, W. Hepples, Influence of voids on damage mechanisms in carbon/epoxy composites determined via high resolution computed tomography, Compos. Sci. Technol. 90 (2014) 147–153.
[13] M. Assarar, D. Scida, A. El Mahi, C. Poilâne, R. Ayad, Influence of water ageing on mechanical properties and damage events of two reinforced composite materials: Flax–fibres and glass–fibres, Mater. Des. 32 (2) (2011) 788–795.
[14] E. Walter, K.H.G. Ashbee, Osmosis in composite materials, Composites 13 (4) (1982) 365–368.

[15] E.E. Shin, R.J. Morgan, J. Zhou, J. Lincoln, R. Jurek, D.B. Curliss, Hygrothermal durability and thermal aging behavior prediction of high-temperature polymer-matrix composites and their resins, J. Thermoplast. Compos. Mater. 13 (1) (2000) 40–57.
[16] M.W. Czabaj, A.T. Zehnder, K.C. Chuang, Blistering of moisture saturated graphite/polyimide composites due to rapid heating, J. Compos. Mater. 43 (2) (2009) 153–174.
[17] D.K. Hsu, D.J. Barnard, J.J. Peters, V. Dayal, Physical basis of tap test as a quantitative imaging tool for composite structures on aircraft, AIP Conf. Proc. 509 (1) (2000) 1857–1864.
[18] V.K. Kinra, A.S. Ganpatye, K. Maslov, Ultrasonic ply-by-ply detection of matrix cracks in laminated composites, J. Nondestruct. Eval. 25 (1) (2006) 37–49.
[19] P.J. Schilling, B.R. Karedla, A.K. Tatiparthi, M.A. Verges, P.D. Herrington, X-ray computed microtomography of internal damage in fiber reinforced polymer matrix composites, Compos. Sci. Technol. 65 (14) (2005) 2071–2078.
[20] F. Awaja, B. Arhatari, K. Wiesauer, E. Leiss, D. Stifter, An investigation of the accelerated thermal degradation of different epoxy resin composites using X-ray microcomputed tomography and optical coherence tomography, Polym. Degrad. Stab. 94 (10) (2009) 1814–1824.
[21] L. Saucedo-Mora, T. Lowe, S. Zhao, P.D. Lee, P.M. Mummery, T.J. Marrow, In situ observation of mechanical damage within a SiC-SiC ceramic matrix composite, J. Nucl. Mater. 481 (2016) 13–23.
[22] A. Abdessalem, S. Tamboura, J. Fitoussi, H.B. Daly, A. Tcharkhtchi, Bi-phasic water diffusion in sheet molding compound composite, J. Appl. Polym. Sci. 137 (7) (2020) 48381.
[23] H.G. Carter, K.G. Kibler, Langmuir-type model for anomalous moisture diffusion in composite resins, J. Compos. Mater. 12 (2) (1978) 118–131.
[24] G. Ibrahim, P. Casari, F. Jacquemin, S. Freour, A. Clement, A. Celino, K. Khalil, Moisture diffusion in composites tubes: Characterization and identification of microstructure-properties relationship, J. Compos. Mater. 52 (8) (2018) 1073–1088.